Journal of Physiology (1991), **442**, *pp.* 147–168
With 7 figures
Printed in Great Britain

THE SPATIAL DISTRIBUTIONS OF ODORANT SENSITIVITY AND ODORANT-INDUCED CURRENTS IN SALAMANDER OLFACTORY RECEPTOR CELLS

BY GRAEME LOWE AND GEOFFREY H. GOLD

From the Monell Chemical Senses Center, 3500 Market Street, Philadelphia, PA 19104, USA

(*Received 17 December 1990*)

SUMMARY

1. Suction electrode and whole-cell recording were used to record membrane currents from defined regions of solitary olfactory receptor cells from *Ambystoma tigrinum*.

2. Under whole-cell current clamp, stimulation of cells with odorants activated an inward current in the cilia, an outward current in the soma, and induced a membrane depolarization. Clamping the membrane potential at its resting value of −70 mV increased the inward ciliary current 5- to 10-fold and abolished the outward somatic current.

3. Local odorant stimulation was accomplished by ejecting an odorant solution into a steady flow of Ringer solution. A suction electrode was used to immobilize a cell in the flow and to record the odorant-induced somatic current. The amplitude of the odorant response increased approximately linearly with the length of cilia exposed to the stimulus, but was independent of the length of dendrite exposed to the stimulus, indicating that odorant sensitivity is predominantly localized to the cilia.

4. The latencies of responses recorded under flow did not vary with the region of the cilia which was exposed to the stimulus. Also, the magnitude of the inward ciliary current activated by odorants was equal to that of the whole-cell current recorded under voltage clamp. These observations indicate that the odorant-induced inward current is predominantly localized to the ciliary membrane.

5. Under whole-cell current clamp, local application of a high-K^+ solution generated an outward somatic current when applied to the dendrite, but had no effect when applied to the cilia. This indicates that the density of the resting K^+ conductance is lower in the ciliary membrane than in the dendritic membrane.

6. The results above are consistent with the hypothesis that all components of the transduction mechanism are uniformly distributed within the cilia, and that the cilia are electrotonically compact, even during an odorant-induced conductance increase.

INTRODUCTION

Vertebrate olfactory receptor cells are distinguished from other neurones by the possession of cilia, which are thought to play a role in the transduction of odorous

stimuli. Morphologically, the cilia are a likely site for transduction to occur because they are the most distal extensions of the receptor cells and also because their small diameter increases the surface area available for binding odorants. However, physiological observations have not established the role of the cilia in transduction. For example, deciliation of the olfactory epithelium has yielded variable results, in some cases causing a large decrease in odorant sensitivity (Bronshtein & Minor, 1977; Adamek, Gesteland, Mair & Oakley, 1984), while in other cases, having little or no effect (Concalon, 1980; Kashiwayanagi, Shoji & Kurihara, 1988). The cause of this variability is not known, in part because the mechanisms and effects of deciliation treatments are poorly understood. However, one explanation may be that part, or all, of the transduction apparatus is contained within the receptor cell dendrite, which might be only partially affected by deciliation treatments. This hypothesis is supported by evidence, based on the latency of the trans-epithelial voltage response to odorants (termed the electro-olfactogram, or EOG (Ottoson, 1956)), that odorant sensitivity is restricted to the apical dendrite or only the basal portion of the cilia (Getchell, Heck, DeSimone & Price, 1980).

More direct observations on the site of olfactory transduction have been provided by recordings of the transduction current in solitary receptor cells in response to focally applied odorants (Kurahashi, 1989; Firestein, Shepherd & Werblin, 1990). Although these studies demonstrated that odorant sensitivity is maximal near the distal end of the receptor cell, the rapid diffusional spread of the stimuli prevented any conclusions regarding the relative contributions of the cilia and dendrite to odorant sensitivity. Nor has it been possible to provide information about the distribution of odorant sensitivity within the cilia. Also, because odorant responses were observed with whole-cell recording, no information has yet been provided about the location of the transduction current in these cells. In view of the evidence that olfactory transduction is mediated by intracellular messengers, the transduction current could originate in the dendrite, even if odorant receptors are confined to the cilia. Because the diameter of the dendrite is larger than that of the cilia, the dendrite might be a more efficient site for initiating an electrophysiological response.

To provide more direct evidence regarding the site of olfactory transduction, we measured the spatial distribution of odorant sensitivity by using rapid perfusion to limit the diffusional spread of the stimulus. We also determined the spatial distribution of the transduction current by simultaneous suction electrode and whole-cell recording. Our results support the hypothesis that olfactory transduction is carried out entirely within the cilia.

METHODS

Preparation

Recordings were made from solitary olfactory receptor cells isolated from terrestrial-phase tiger salamanders (*Ambystoma tigrinum*). Animals were killed by decapitation and pithing, and the olfactory epithelium was excised as a sheet (dorsal or ventral) and cut into slices with a razor blade. Solitary cells were obtained by two methods of dissociation. In some experiments the tissue was exposed to a low-calcium citrate buffer at pH 10·3 for 45 min (Kleene & Gesteland, 1983). In others, the tissue was treated with Trypsin (Sigma; 1 mg ml^{-1} with 0·5 mM-EGTA, 0 Ca^{2+}, for 20 min); followed by DNase Type I or II (Sigma; 0·1 mg ml^{-1} for 10 min). Similar results were obtained with both techniques. Cells released by triturating slices with a pasteur pipette were allowed to settle

onto a cover-slip mounted on the bottom of an open plexiglass dish, and examined under phase contrast and differential interference contrast on a Zeiss Axiovert 35M microscope, equipped with a Plan-Neofluar objective (40 ×). Unused slices were stored at 4 °C and remained viable for several hours. Immediately after trituration, receptor cells could be identified by the presence of an elongate dendrite, at the tip of which were several motile cilia 20–30 μm long. The lengths of the cilia on solitary cells were representative of the lengths of cilia observed along the edges of epithelial slices. With increasing time after trituration, the dendrites of most cells were slowly absorbed by the somata, and the cells became nearly spherical. The cilia, however, did not appear to be absorbed into the dendrite and soma, since cilia were often observed extending from otherwise spherical cells. Electrophysiological responses to odorant stimulation were similar in cells with and without elongate dendrites, and therefore we did not select for cells with elongate dendrites unless it was necessary for a particular experiment. Dissection, washing, storage and recording were done in an amphibian Ringer solution (Bader, MacLeish & Schwartz, 1979) containing (in mM): NaCl, 85; $NaHCO_3$, 1; NaH_2PO_4, 0·5; sodium pyruvate, 1; KCl, 1·5; $MgCl_2$, 0·5; $MgSO_4$, 0·5; $CaCl_2$, 1·8; D-glucose, 16; Na-HEPES, 10; 0·001 % Phenol Red (sodium salt); pH = 7·4. All dissociations and experiments were done at room temperature (23 °C).

Electrodes and recording

The methods for suction electrode recording were essentially the same as those used by Baylor, Lamb & Yau (1979) and the methods for whole-cell recording followed those of Hamill, Marty, Neher, Sakmann & Sigworth (1981). Recording electrodes were fabricated from 100 μl borosilicate glass capillary pipettes (Drummond Scientific Co.) using a Model P-87 Flaming-Brown micropipette puller (Sutter Instrument Co.). Tips were fire-polished to final inner diameters of 8–10 μm for suction recording from cell bodies (resistance 0·4 MΩ), and 3–4 μm for suction recordings from cilia (resistance 0·8 MΩ). We did not measure the diameters of the tips of whole-cell pipettes but the resistances were 4–6 MΩ. Suction electrodes contained amphibian Ringer solution, and whole-cell electrodes were filled with a solution containing (mM): KCl, 50; potassium aspartate, 50; $MgCl_2$, 5; $NaHCO_3$, 1; $MgSO_4$, 1; K_4EGTA, 0·1; HEPES (potassium salt), 5; Na_2ATP, 5; Na_3GTP, 1; 0·001 % Phenol Red (sodium salt); pH = 7·2. All electrode solutions were filtered before use (Millex-GV_{13}, 0·22 μm, Millipore Corp). A Ag–AgCl pellet was used for both bath and recording electrodes.

Signals were recorded with a Yale Mark V patch-clamp amplifier, and passed through an 8-pole Bessel filter before being digitized for analysis on a PDP 11/23 computer with an INDEC analog interface. Pipette and seal resistances were monitored by applying negative voltage pulses and recording the resulting current. The pipette potential was held at zero during suction electrode recording.

Collection efficiency of the suction electrode

Due to the low resistance shunt caused by the cell-electrode seal, the patch-clamp amplifier detects only a fraction, α, of the total current flowing through the membrane enclosed by the suction electrode. If this membrane is restricted to the tip of the electrode, then

$$\alpha = \frac{R_S}{R_S + R_P}, \tag{1·0}$$

where R_S is the cell-electrode seal resistance and R_P is the pipette series resistance (Stuhmer, Roberts & Almers, 1983). However, if parts of the cell membrane extend into the suction electrode, the effective series resistance is decreased and the effective seal resistance is increased, resulting in more efficient collection of the membrane current.

For recording from the soma, we used electrodes with steeply tapered tips (90–115°). In such experiments (e.g. Figs 3 and 5), most of the somatic membrane bypassed the first few micrometres of the tip, which contained about 75 % of the total series resistance (estimated from the observed profile of the electrode). This reduced the effective series resistance by about 4-fold, allowing the patch-clamp amplifier to detect most of the membrane current. With measured seal resistances of 2–6 MΩ, and total series resistances of 0·4–0·6 MΩ, we estimated that α would be larger than 0·90.

For recording from cilia, we used less steeply tapered electrodes. We calculated α by modelling the ciliary bundles as a distributed current sink within the pipette, and summing the contributions to the suction electrode current arising from cross-sectional slices of this volume located at different

points along the axis of the pipette. If the current sinks are distributed along the cilia with a normalized density $\phi(x)$ at an axial distance x from the tip of the pipette, and if the dendritic patch contributes a fraction δ to the total current, then α is given by the following formula:

$$\alpha = \frac{R_S}{R_S+R_P} + \frac{(1-\delta)\rho}{(R_S+R_P)\pi}\int_0^L \phi(l)\int_0^l \frac{dx\,dl}{f(x)^2}, \tag{1·1}$$

where L is the length of the ciliary bundle, ρ is the resistivity of the Ringer solution (measured value 118 Ωcm), and the function f is the inner radius of the suction electrode (approximated by a piecewise linear function, with parameters measured by light microscopic inspection of electrodes using an eyepiece reticule). For L we used a visually estimated mean ciliary length. In the calculations where we assumed an equal density of current in both the cilia and the patch of dendritic membrane at the base of the cilia, we took $\delta = A_P/(A_P+A_C)$, where A_P is the area of the dendritic patch (estimated visually), and A_C is the surface area of the part of the cilia assumed to act as a current sink (assuming a diameter of 0·25 μm (Reese, 1965)).

Odorant stimulation in a stationary solution

Cells were transiently stimulated by a mixture of odorants dissolved in Ringer solution. The solution was ejected from a micropipette by pressure pulses (14–103 kPa, 20–100 ms) applied through a computer-controlled solenoid valve. The tip geometry of the stimulus micropipette was similar to that of the whole-cell micropipettes. Stimuli were visualized by adding a dye (0·3% Bromophenol Blue, sodium salt) to the odorant solution. The initial diameter of the stimulus depended on pulse pressure and duration (typically 20 μm at 28 kPa, 20 ms) and spread rapidly due to diffusion, as indicated by the disappearance of the dye within *ca* 250 ms after the end of the pulse. The mixture of odorants contained some or all of the following: 2-hexylpyridine (Oxford Chemicals, UK), isoamyl acetate, acetophenone, and cineole (Aldrich). A mixture of odorants was used to increase the probability of eliciting responses from cells selected at random. Odorant solutions were prepared by mixing each odorant with the amphibian Ringer solution to give a total nominal concentration of 10 mM, and waiting 2–3 h for equilibration. The stimulus solution was then prepared by mixing equal volumes of these solutions and passing the mixture through a millipore filter (Millex GV_{13}). Although not measured, the total odorant concentration in the stimulus micropipette must have been lower than 10 mM because a hydrophobic phase was observed on the surface of the solution before filtration.

In some experiments (e.g. Figs 3 and 5), the odorant solutions were made in a high-K^+ solution with 85 mM-KCl substituted for 85 mM-NaCl in the amphibian Ringer solution. The high K^+ caused an immediate transient current, beginning less than 20 ms after the voltage pulse was applied to the solenoid valve. This current provided an approximate indication of the time course of the odorant stimulus (Firestein & Werblin, 1989). During whole-cell recording under voltage clamp, the K^+-induced current was a transmembrane current caused by a change in the driving force for K^+ across the membrane. However, during suction electrode recording when the stimulus was applied near the electrode tip (e.g. Fig. 5*B*), the high K^+ may have also induced a liquid junction current across the low-resistance membrane–electrode seal. As both the membrane current and the liquid junction current had similar time courses, we did not attempt to distinguish between them. We did not use the K^+ current to estimate the absolute concentration of odorant reaching the cell, as was done by Firestein & Werblin (1989). However, the similarity of our stimulus geometry to theirs suggests that the peak odorant concentration reaching the cells was 10–100 μM.

Odorant stimulation in a flowing solution

A continuous flow of Ringer solution was maintained over a cell held in a suction electrode by positioning the cell approximately 100 μm from the tip of a glass capillary tube (i.d. 50 μm), fed from an elevated reservoir. Odorant stimulation was accomplished by positioning the tip of the stimulus micropipette close to the cell and ejecting a transient plume of odorant solution (prepared as above). By choosing a sufficiently high flow rate, the spread of odorant longitudinally upstream from the stimulus pipette, and laterally downstream in the plume, could be made small relative to the dimensions of the cell. If D is the diffusion coefficient of the odorant, U, the flow velocity, and L the length scale of the dendrite and cilia, then we required: $U \gg 4D/L$. For $D = 6\times10^{-6}$ cm^2 s^{-1} (Getchell *et al.* 1980) and $L = 25$ μm, $U \gg 100$ μm s^{-1}. We found that dendrites were able to withstand flow rates as high as 2000 μm s^{-1} without separating from the soma. The plume was

visualized with dye as a dark region with a relatively sharp boundary (Fig. 2) which appeared linear and uniform in width for at least 150 μm downstream from the tip of the stimulus pipette, indicating that the diffusional spread of the dye was reduced by the high flow rate. Although the odorants we used have a lower molecular weight (120–163 g mol^{-1}) than the dye (670 g mol^{-1}), their diffusion coefficients (estimated from molecular weight) are only about twice as large, so that convective transport was still expected to dominate. We therefore expected the dye boundary to be a reliable indicator of a boundary in odorant concentration.

The stimulus solutions contained high K^+, and the K^+ concentration in the centre of the plume was estimated by measuring the liquid junction current generated in a fine-tipped micropipette. This measurement showed that the K^+ concentration (and therefore the odorant concentration) in the plume was not significantly diluted relative to that within the stimulus micropipette. A high odorant concentration was needed to elicit measurable responses when stimulating only a fraction of the cilia with stimuli of short duration. There was no evidence for non-specific effects of the odorants, since only a small fraction of the cells responded to the odorants under these conditions, whereas nearly all cells responded to high K^+.

A plume ejected from a point along the mid- or basal part of the dendrite usually enveloped all parts of the cell located downstream from the stimulus pipette. However, when the point of ejection was positioned near the tip of the dendrite, or in the region of the ciliary bundle, the dendrite and cilia were deflected by the plume. Therefore, a video camera and a videocassette-recorder were used to record the location of each stimulus relative to the cell, and frame-by-frame analysis was later used to determine the region of the cell enveloped by the plume. The outline of the cell and the boundary of the plume were traced from the Normarski image displayed on a video monitor; the boundary of the plume was defined by estimating where the image intensity was midway between the background intensity and the intensity at the centre of the plume. In cases where the boundary was not perpendicular to the axis of the dendrite or ciliary bundle, we computed its average position from the two points of intersection with the outline of the dendrite or ciliary bundle. The flow velocity at various positions was determined by tracing the motion of small particles (diameter < 2 μm) between successive video frames.

In some cells the amplitude of the odorant response decayed significantly during the course of an experiment. To compensate for this, the maximal response was measured periodically, and was used to scale responses at intermediate times, assuming that all parts of the cell decayed at the same rate. In some cells the dendrite contracted slowly, and we compensated for this by rescaling stimulus positions relative to the location of the tip of the dendrite. The cilia were never observed to contract.

RESULTS

Odorant-induced current recorded in the soma

The trace in Fig. 1*B* shows a typical somatic current recorded in response to a brief odorant stimulus which completely enveloped the cilia and the exposed dendritic and somatic membrane. In this cell, the dendrite was completely absorbed into the soma prior to recording; similar responses were observed in the somata of cells in which the dendrite remained elongate and only the somatic membrane was held within the suction electrode (e.g. Figs 3 and 5*A*). The current was outward with a peak amplitude of 44 pA. Since the suction electrode enclosed only about one half of the somatic membrane (Fig. 1*A*), the total somatic current should have been about 90 pA. The odorant-induced somatic current was outward in polarity for all cells in which an odorant response was detectable ($n > 200$; detection threshold *ca* 5 pA without signal averaging). This implies that, neglecting capacitative current, there is an equal net inward current through the cell surface outside the suction electrode, which includes the ciliary and dendritic membranes. We shall call this inward current the transduction current, whether it is measured under current clamp or voltage clamp.

The peak amplitude of the somatic current responses varied from cell to cell, the largest observed being 150 pA. The fraction of cells which exhibited a detectable response to the odorant mixture used (see Methods) was as large as 60% in some preparations, but was frequently much lower. The duration of an odorant response

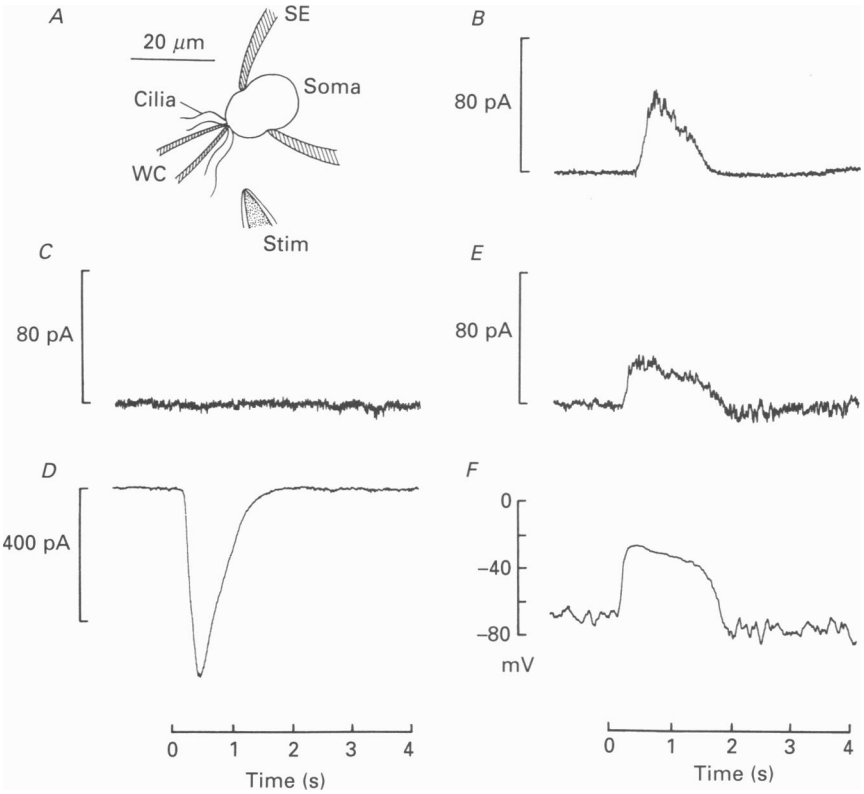

Fig. 1. Analysis of the odorant-induced somatic current by simultaneous suction electrode and whole-cell recording. *A*, shows a video-tracing indicating the positions of the cell, electrodes (SE, suction electrode; WC, whole-cell electrode) and stimulus pipette (Stim). *B*, shows the suction electrode current recorded from the cell before breakthrough with the whole-cell electrode. After breakthrough, the membrane voltage was clamped at −70 mV, and both the suction electrode current (*C*) and whole-cell current (*D*) were recorded. The whole-cell current was then clamped to zero, and the suction electrode current (*E*) and whole-cell voltage (*F*) were recorded. In this and other figures, a current directed out of the cell membrane is taken as positive, and the time scale for each trace is drawn so that zero time coincides with the initiation of the signal which triggered stimulus ejection. In this experiment, the stimulus was ejected by a 34 kPa pulse of 30 ms duration. We obtained similar data from two other cells in this recording configuration.

was also variable (0·9–7·1 s at the detection threshold for a pulse duration of 20 ms), as was the latency (50–400 ms, as determined by the intersection with the baseline of the tangent to the inflection point on the rising phase of the response). The variability in the amplitude and time course of the odorant responses may have reflected the physiological state of the cells as well as the heterogeneity of

olfactory receptors, which could include differences in both odorant specificity and transduction kinetics.

To investigate the mechanism underlying the somatic current, we recorded this current while simultaneously clamping or measuring the membrane potential with a whole-cell patch-clamp electrode (Hamill *et al.* 1981). Figure 1*C–F* shows odorant responses from the cell of Fig. 1*A* and *B* after the whole-cell configuration was obtained with a second microelectrode. When the membrane voltage was clamped at −70 mV a large inward current (amplitude 560 pA) was detected by the whole-cell electrode in response to odorant stimulation (Fig. 1*D*). By contrast, the suction electrode current was eliminated during voltage clamp (Fig. 1*C*). These observations demonstrate that the outward somatic current was caused by odorant-induced depolarization of the cell. This interpretation was confirmed by simultaneous measurements of the somatic current and membrane potential under current clamp (Fig. 1*E* and *F*); a large depolarization (40 mV) occurred simultaneously with the somatic current. In other cells inward current spikes (1·3–2·2 ms duration at half-maximal amplitude) were superposed on the rising phase of the outward somatic current, indicating the occurrence of action potentials. The longer time course and shorter latency of the suction electrode current during whole-cell recording compared with that seen before breakthrough, and the noisier baseline under both current and voltage clamp, were probably due to cell dialysis.

The current noise at the peak of an odorant response recorded with the suction electrode was often many times larger than the baseline noise level (Fig. 1*B*). This increase in noise was most likely due to the opening of voltage-activated channels and not odorant-regulated channels, because it was not seen in the whole-cell current recorded under voltage clamp (Fig. 1*D*). Under current clamp, the voltage showed baseline fluctuations of order 8 mV at the resting potential of −70 mV (Fig. 1*F*). These voltage fluctuations were correlated with the inward current fluctuations in Fig. 1*E*, which must therefore have been due to channels in the somatic membrane. During the peak and plateau phase of the odorant response, voltage fluctuations were suppressed, indicating a substantially lower input resistance (less than 100 MΩ at peak, estimated from the ratio of voltage noise to current noise). In most experiments the current noise increased after breakthrough with the whole-cell pipette, so the resting baseline voltage of intact cells is probably less noisy than in Fig. 1*F*.

Spatial distribution of odorant sensitivity

To determine the spatial distribution of odorant sensitivity, the somatic current was recorded with a suction electrode while an odorant stimulus was injected into a flowing stream of Ringer solution, as described in Methods (Fig. 2). In addition to creating a linear plume and limiting the diffusional spread of the stimulus, the flow also served to align the dendrite and cilia along a single axis, so that the stimulus geometry was approximately one-dimensional.

Figure 3 shows a series of responses to stimuli of 50 ms duration recorded from a cell as the boundary of the plume was progressively moved upstream in the flow, to envelop the cilia and then the dendrite. Each trace represents the average of four successive responses to stimuli delivered every 8–10 s; odorant stimulation at this

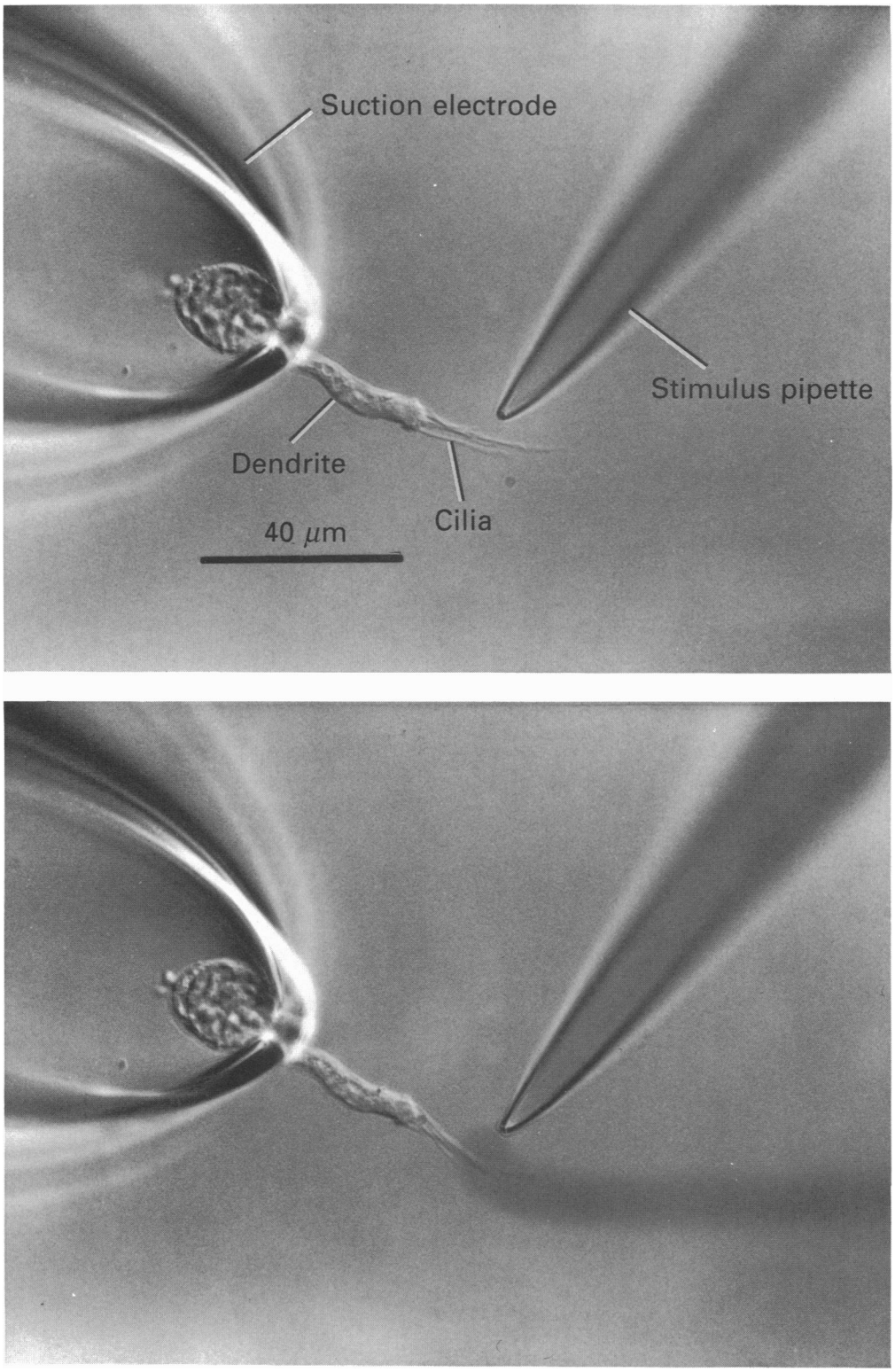

Fig. 2. For legend see facing page.

frequency did not cause any desensitization. The downward spikes on the rising phase of each response represent action potentials which were reduced in amplitude by the signal averaging. The peak amplitude of the odorant response increased as the ciliary bundle was enveloped by the plume, but did not increase further when the dendrite was enveloped. The brief outward current which preceded the odorant response in the lower traces was caused by the high K^+ in the stimulus solution.

In Fig. 4*A* the peak amplitudes of the odorant-induced current (○) and the K^+-induced current (●) recorded from the cell of Fig. 3 are plotted as a function of the position of the plume boundary. The outline of the cell is drawn to reveal the relationship between the electrophysiological response and the region of the cell exposed to the stimulus (dashed line). The plot shows that the odorant response increased linearly with the length of the cilia enveloped by the stimulus, but remained approximately constant at its maximal value as the stimulus enveloped an increasing length of the dendrite. The small decrease in the odorant response when the edge of the plume was moved proximally along the dendrite in some cells (e.g. Fig. 4*A* and *B*), was probably due to deflection of the odorant plume by the dendrite. The point of transition between the rising phase and the plateau for these data, as determined by the intersection of the two straight lines fit by eye to the data points, is within a few micrometres of the tip of the dendrite. Also, the distal limit of the odorant-sensitive region, defined by extrapolating the straight line to zero amplitude, was near the tip of the ciliary bundle.

Data from three other cells are shown in Fig. 4 to illustrate the cell-to-cell variations in these measurements. In all cases, the odorant-sensitive region, i.e. the region of negative slope, coincided approximately with the ciliary bundle, and the slope of the odorant–response plots was approximately constant in the sensitive region. Although in some cases the odorant-sensitive region appeared to overlap the tip of the dendrite (Fig. 4*B* and *D*), this does not necessarily imply that the tip of the dendrite is odorant sensitive. For example, variations in the absolute sensitivity of single cells would be expected to produce variations in the position, with respect to the visible edge of the plume, where each cell locally produced its maximum response. Also, the odorant-sensitive region might appear to overlap the tip of the dendrite if the points of origin of the cilia were displaced proximally from the tip of the dendrite, as occurred in the cell in Fig. 7*B*. The length of the odorant-sensitive region tended to underestimate the observed length of the ciliary bundle. Although this could indicate lower odorant sensitivity near the tips of the cilia, there are two reasons why these measurements would produce such an underestimate. First, inspection in the light microscope would have been more likely to miss shorter cilia, which were obscured by the ciliary bundle, than longer cilia, which protrude from the bundle. Thus, the drawings in Fig. 4 probably reflect an overestimate of the mean length of the cilia. Second, ciliary motility and deflection of the cilia by the stimulus plume would have caused an underestimate of sensitivity near the tips of the cilia.

Fig. 2. Photomicrographs (taken under Nomarski optics) of an olfactory receptor cell under rapid perfusion. In the upper picture, the stimulus plume was switched off, and in the lower picture it was switched on and enveloped the distal half of the ciliary bundle. The direction of flow was from left to right.

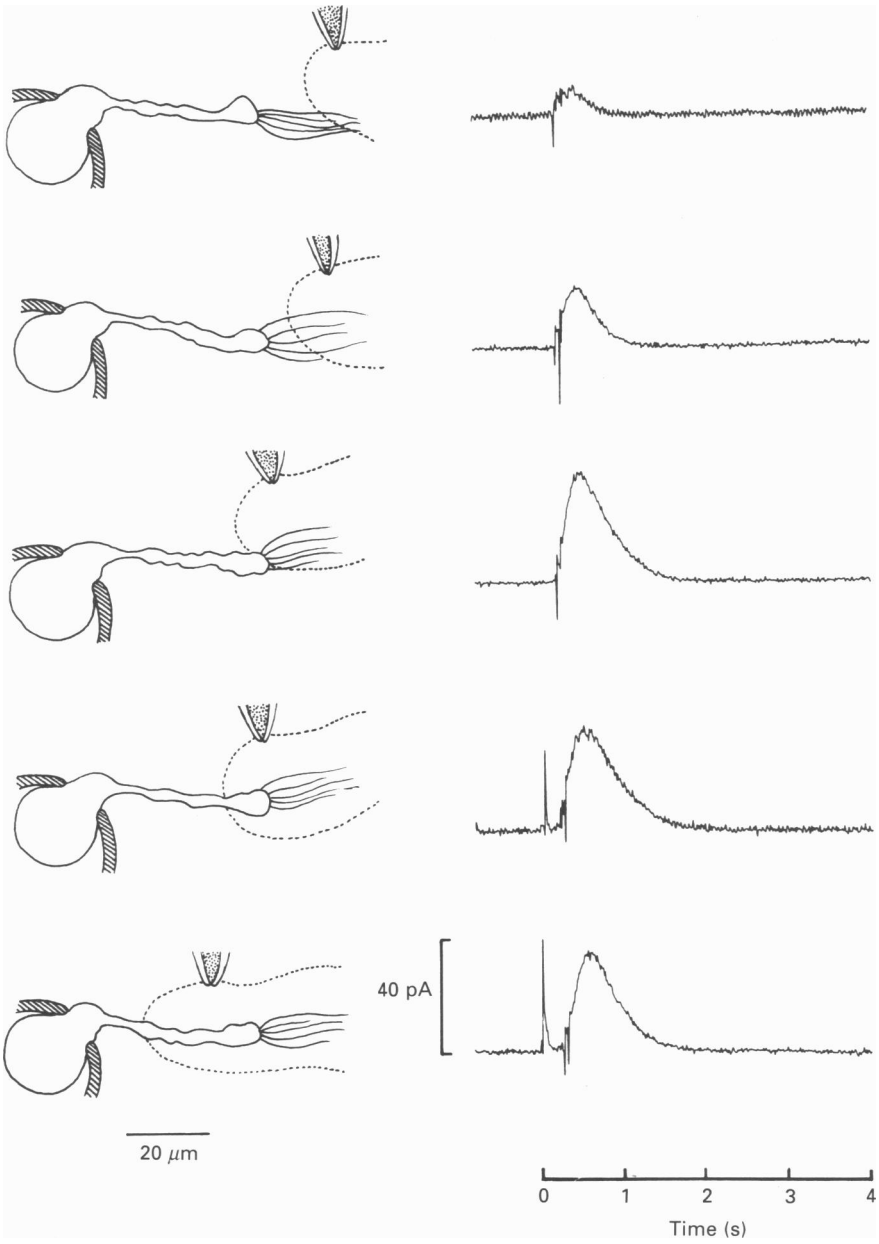

Fig. 3. Mapping of odorant sensitivity by local stimulation with perfusion. Each trace on the right shows the somatic current recorded for the stimulus geometry shown in the corresponding video tracing on the left. The direction of flow was from left to right. The flow rate was 420 ± 50 μm s^{-1} in the vicinity of the cilia, and 950 ± 50 μm s^{-1} along a streamline 10 μm from the surface of the dendrite. The duration of each stimulus was 50 ms.

In interpreting these data, we assumed that the increase in response amplitude reflected an increase in the length of the cilia which were exposed to the bulk odorant concentration in the plume. Strictly, the observed response profile is a convolution

of the stimulus concentration profile with the concentration–response function at each point along the cilia. However, the close agreement between the limits of the odorant-sensitive region and the morphological limits of the ciliary bundle, as well as the approximately linear dependence of response amplitude on plume position, argue

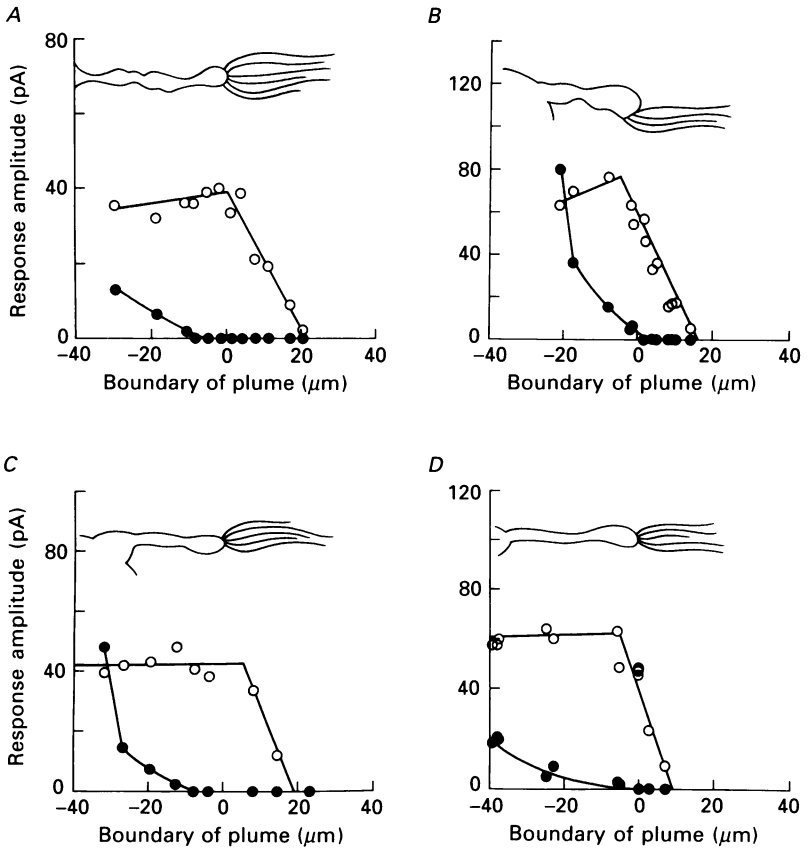

Fig. 4. The amplitudes of the responses to odorant (○) and potassium (●) recorded under perfusion for four different cells, plotted as a function of the position of the leading edge of the stimulus plume. A piecewise linear function was fitted by eye to the data for the odorant response. Each panel shows data obtained from one cell, whose outline is drawn to the same scale as the horizontal axis. The cells and their ciliary bundles were drawn from phase-contrast and Nomarski images recorded on videotape. Due to the difficulty in resolving the cilia under these conditions, the drawings only approximately reflect the number (±2) and lengths (±4 μm) of the individual cilia. The data in panel *A* were obtained from the cell of Fig. 3. The flow rates and the distances from the dendrite where the flow measurement was made, were: *B*, 820±50 μm s^{-1}, 8·5 μm; *C*, 1830±120 μm s^{-1}, 7 μm; *D*, 2190±100 μm s^{-1}, 9 μm. Stimulus durations were 100 ms for cells in *B*, *C* and *D*. For the cells in *A*, *B* and *C* there was no decay in the amplitude of the odorant response, and no dendritic contraction during the measurements shown. For the cell in *D*, the amplitude decayed to 70% of its initial value, and the dendrite contracted to 95% of its initial length in 5 min. Similar data were obtained from two other cells.

that the stimulus approximated a step function in space and that the observed response profile reflects spatial summation by the cilia. This conclusion is further supported by the fact that the time course of the responses was independent of the

stimulus position (Fig. 7*A*); if the maximal response amplitude reflected saturation of the transduction mechanism, we would have expected to see an increase in response duration, such as occurred in the cell in Fig. 5 when the stimulus was applied directly to the cilia. It may be surprising that the somatic current did not appear to saturate with the high stimulus concentration in the plume (close to 10 mM) since solitary cells have been reported to saturate at stimulus concentrations of approximately 300 μM (total odorant concentration (Firestein & Werblin, 1989)). However, this is most likely due to the shorter stimulus duration in our experiments with a flowing solution (an approximately square pulse, 50 ms long), compared with that used by Firestein and Werblin (a truncated exponential with a time constant of several hundred milliseconds).

Spatial distribution of the resting K^+ conductance

The response to the high K^+ in the stimulus plume provided information about the spatial distribution of the resting K^+ conductance. The K^+ response was never observed when the stimulus was limited to the ciliary region, but became detectable as the plume enveloped a significant fraction of the dendrite. Since the ability of a rise in extracellular K^+ to depolarize the cell depends on the density of K^+ channels which are open at the resting potential, our data indicate that the resting K^+ conductance per unit area is lower in the cilia than it is in the dendrite. We placed an upper bound on the ratio, Θ, of the density of the ciliary to the dendritic K^+ channels as follows. If the cilia and the dendrite are assumed to be electrotonically compact and to contain uniformly distributed K^+ conductances, then the inward K^+ current is proportional to the membrane area enveloped by the plume, and the measured outward K^+ current is proportional to the fraction of the remaining membrane area enclosed by the suction electrode. The observation of no current when the cilia were enveloped, and of a finite current when part of the dendrite was enveloped, gave two conditions allowing us to eliminate the unknown proportionality constants and compute the ratio of channel densities. If I_T is the threshold current detectable by the suction electrode, I_M the measured K^+ current when a length, l_D, of the dendrite is enveloped by the plume, and if the cilia and dendrite are modelled as cylinders of radii r_C and r_D, then:

$$\Theta \leqslant \frac{r_D l_D}{N r_C L_C} \frac{I_T}{I_M - I_T}, \tag{2·0}$$

where N is the number of cilia and L_C is the mean ciliary length. For the cell of Fig. 3, we took $I_T = 1{\cdot}3$ pA (the noise level of an averaged current trace), $I_M = 24$ pA, $L_C = 30\ \mu$m, $N = 6$, $l_D = 35\ \mu$m, $r_D = 2{\cdot}2\ \mu$m, $r_C = 0{\cdot}125\ \mu$m (Reese, 1965), and obtained $\Theta \leqslant 0{\cdot}20$; i.e. the density of the resting K^+ conductance is at least 5-fold lower in the cilia than in the dendrite.

The spatial distribution of the transduction current

The data in the previous section showed that odorant sensitivity is concentrated in the cilia. If the receptive sites were directly linked to the ion channels which carry the transduction current, then this current would also be limited to the ciliary membrane. However, in view of the evidence that olfactory transduction is mediated

by diffusible second messengers, some or all of these channels could be located in the apical dendritic membrane. To investigate this possibility, we measured the transduction current under whole-cell voltage clamp, while recording the ciliary and dendritic current with a suction electrode.

Stimulating the cilia within the suction electrode

Measuring the odorant-induced current in the cilia and dendrite required a method for stimulating the cilia while they were enclosed by the suction electrode. This was accomplished by applying odorants outside the suction electrode and allowing them to reach the cilia by diffusing through the cell. Evidence that the cilia may be stimulated in this way is provided below.

Figure 5 shows the responses obtained from a cell with the suction electrode recording either the somatic current or the ciliary and dendritic current. The stimulus (2-hexylpyridine in the high-K^+ Ringer solution) was ejected into a stationary solution and allowed to dissipate by diffusion. The upper trace was recorded with the soma held in the suction electrode, and the stimulus applied directly to the cilia. In this configuration the odorant elicited an outward somatic current (amplitude 80 pA, latency 100 ms). There was no response to the high K^+ presumably because the stimulus was centred on the cilia where the resting K^+ conductance is low (see above). The cell was then ejected from the suction electrode and drawn in with only the somatic membrane exposed (Fig. 5, lower trace). In this configuration a response to the high K^+ was observed (the initial upward transient), followed by an odorant response of the opposite polarity. In view of the evidence described above that odorant sensitivity is restricted to the cilia, we conclude that in both configurations the responses were mediated by odorant receptors in the cilia activating an inward current in the apical part of the cell. The longer latency and reduced amplitude in the lower trace (1·2 s, 40 pA) would then reflect the greater distance and diffusion barriers between the stimulus micropipette and the cilia.

In the lower configuration, the odorant could have gained access to the cilia either by diffusing through the low resistance seal between the cell membrane and the electrode, or by crossing the membrane and cytoplasm. To distinguish between these two possibilities, we recorded the odorant response from a cell in this configuration before and after the formation of a gigaohm seal with the suction electrode. A gigaohm seal should eliminate diffusion through the paracellular pathway (Hamill *et al.* 1981). We found that seal formation reduced the amplitude of the response from 26 to 7 pA. This reduction may have been due to elimination of the paracellular pathway, but may also have been caused by damage to the membrane within the suction electrode, since this part of the cell changed shape rapidly during seal formation. However, the detection of an odorant response after gigaohm seal formation demonstrated that odorants could reach the cilia by diffusing through the membrane.

Determining the distribution of the transduction current

The ability to stimulate cilia within the suction electrode allowed us to investigate the spatial distribution of the transduction current as follows. In Fig. 6*A*, the cilia and a portion of the dendrite of a cell were pulled into the tip of a suction electrode

and then whole-cell recording was established with a second microelectrode. Under voltage clamp, odorant stimulation induced a transient inward current which was detected by both the whole-cell electrode and the suction electrode. Stimuli were presented with the tip of the stimulus pipette at the three positions shown. As the tip was moved away from the cilia, the latency of the response increased and the

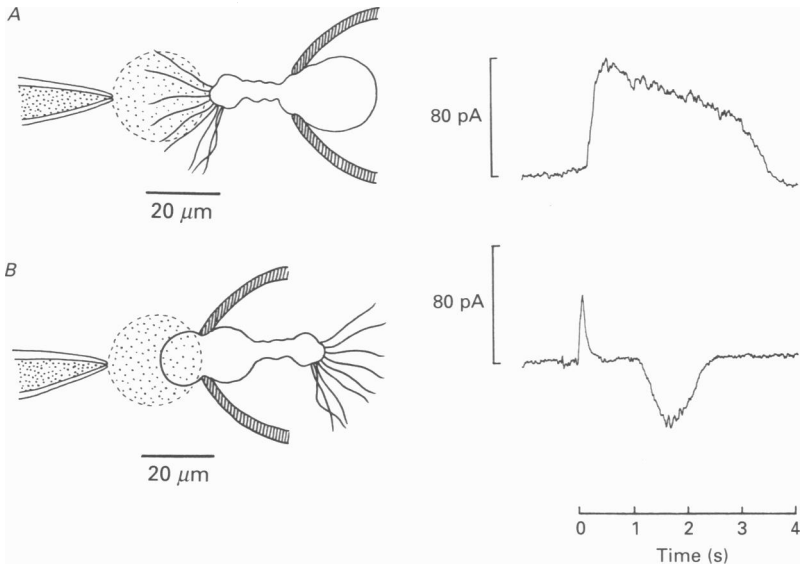

Fig. 5. Suction electrode responses of a single cell to 2-hexylpyridine with the cilia outside (*A*) and inside (*B*) the suction electrode. Stimuli were ejected by 100 ms pressure pulses. The drawings at left illustrate the recording geometries and approximate initial extent (stippled area) of the ejected stimulus.

amplitude decreased. This confirmed that the responses were due to the odorants acting on the cilia rather than on the basal somatic membrane. At each stimulus position, the suction electrode and whole-cell currents were identical in amplitude and time course, demonstrating that the transduction current originated entirely from the membrane within the suction electrode. This membrane included not only all of the cilia, but also the apical part of the dendrite. However, it is unlikely that the dendrite contributed significantly to the suction electrode current because of the sharply decreased collection efficiency in the terminal constriction where the dendritic membrane was located. Using estimates of 0·5 MΩ for R_S and 0·7 MΩ for the effective value of R_P, eqn (1·0) predicts that only *ca* 40% of the dendritic current would have been detected. This implies an upper limit of *ca* 0·1 on the fraction of the whole-cell current which could have originated in the dendrite (based on the minimum resolvable difference between the suction electrode and whole-cell currents).

To study the distribution of the transduction current in more detail, we recorded from cells in which the dendritic membrane did not protrude into the suction electrode, so that the proximal portions of the cilia occupied the terminal region of the electrode (Fig. 6*B*). In this configuration, the suction electrode should detect only a fraction of the ciliary current. As expected, the suction electrode current, I_S, was

smaller than the whole-cell current, I_{WC}, by a constant scale factor which varied between 0·50 and 0·85 for different cells (depending on the seal resistance and electrode shape). Comparing this factor with the collection efficiency α, calculated

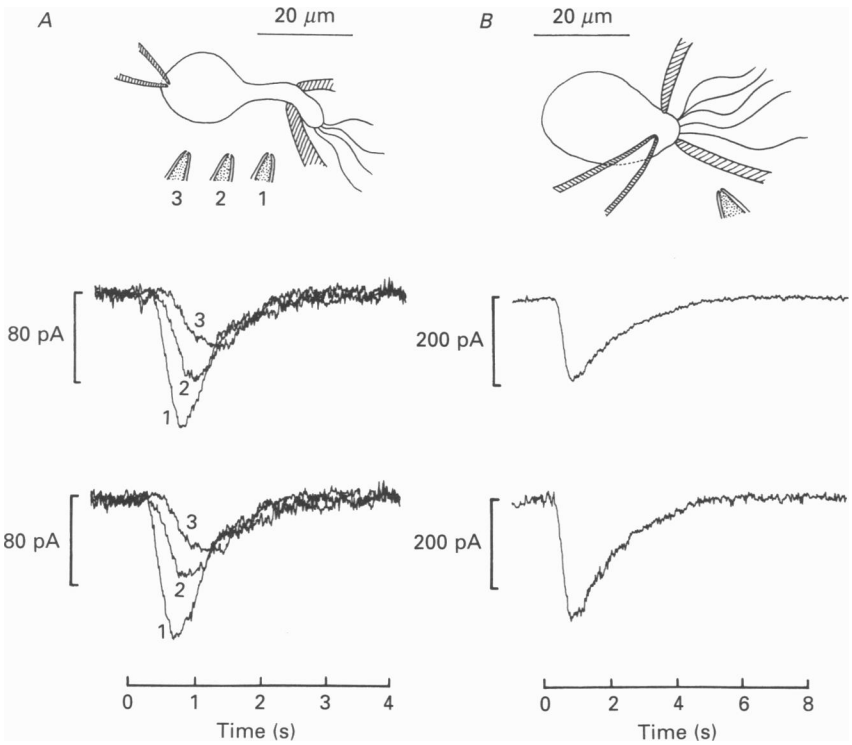

Fig. 6. Suction electrode recordings of odorant-induced ciliary currents during whole-cell voltage clamp. The traces in *A* show the suction electrode currents (upper traces) and whole-cell currents (lower traces) recorded from a cell with an elongate dendrite; the three traces in each plot (numbered 1–3) correspond to the three numbered positions of the stimulus pipette in the video tracing. The input resistance was 1·0 GΩ. Stimuli were applied with 21 kPa pressure pulses of 40 ms duration. The two plots are superimposable, i.e. the suction and whole-cell currents are identical in time course for all stimulus positions. The traces in panel *B* were obtained from a rounded cell (cell 1 of Table. 1) in which the base of the ciliary bundle was located at the tip of the suction electrode (as shown in the video tracing); they show the suction electrode current (upper trace) and the whole-cell current (lower trace) recorded with the membrane voltage clamped to −70 mV. When the suction electrode current is rescaled to the same peak amplitude as the whole-cell current, both have the same time course. The input resistance of this cell was 1·8 GΩ. Stimuli were applied with 103 kPa pulses of 70 ms duration, using a stimulus pipette with a series resistance of about 10 MΩ.

using eqn (1·1), allowed us to test the validity of several hypothetical current distributions in the ciliary and the dendritic membrane.

We computed α for current distributions in which the ciliary current density, $\phi(x)$, was constant and non-zero only from the bases of the cilia out to a fraction, β, of the total ciliary length, and with or without an equal current density in the dendritic membrane. In Table 1 α is compared with the observed ratio I_S/I_{WC} for three cells.

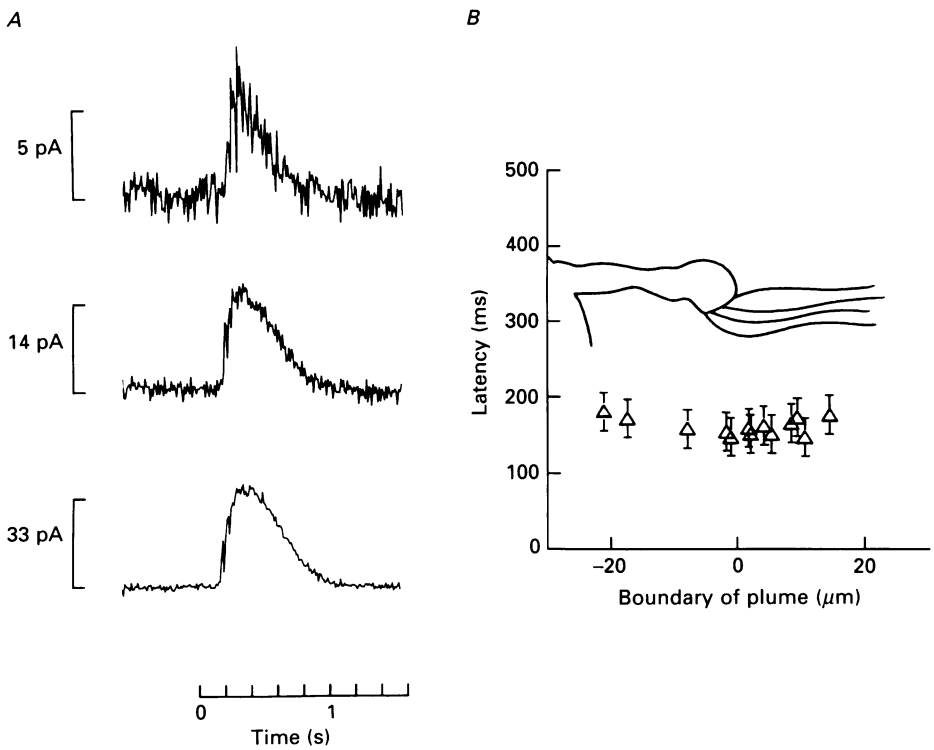

Fig. 7. Dependence of the latency and time course of the odorant response on the position of the stimulus plume. The traces in *A* show the odorant responses recorded at three positions along the cilia of the cell of Fig. 4*B* (from the upper to the lower trace, the distances from the tip of the dendrite were 14, 8 and 5 μm). The traces have been scaled to the same peak amplitude to show the similarity in time course. Each trace represents the average of several consecutive responses (from top to bottom, six, five and four responses). In panel *B*, the latency is plotted as a function of the distance of the edge of the plume from the tip of the dendrite. Similar results were obtained for the other cells in Fig. 4. In cells with longer dendrites, the latency was also constant along the dendrite.

TABLE 1. Comparison of the observed values of I_S/I_{WC} with those predicted (α)

		α				
Cell no.	I_S/I_{WC}	$\beta = 0{\cdot}0$	$\beta = 0{\cdot}1$	$\beta = 0{\cdot}2$	$\beta = 0{\cdot}5$	$\beta = 1{\cdot}0$
1	0·68		0·53	0·58	0·66	0·70
		(0·41)	(0·42)	(0·43)	(0·48)	(0·54)
2	0·50		0·37	0·41	0·46	0·50
		(0·29	(0·30)	(0·31)	(0·35)	(0·39)
3	0·83		0·72	0·78	0·86	0·92
		(0·60)	(0·63)	(0·67)	(0·76)	(0·84)

Values of α were calculated from several assumed distributions of current sinks in the cilia and dendrite. The values without parentheses assume that the current is limited to the cilia; those with parentheses assume an equal current density in the cilia and dendrite. Values of δ for these cells were: 1, 0·55; 2, 0·48; 3, 0·25. Estimated mean ciliary lengths were 25 μm for all three cells. Similar observations were made on five other cells.

The estimated error in α was 0·1, determined by inserting the difference between the measured and calculated values of the pipette series resistance into eqn (1·1). The deviation between α and I_S/I_{WC} was greatest when the current was assumed to arise entirely from the dendritic membrane ($\beta = 0$), and was still significant if the current was localized to the basal 20% of the length of the ciliary bundle. For distributions over larger fractions of the ciliary length ($\beta \geqslant 0{\cdot}5$), α did not differ significantly from the measured ratio. This reflects the fact that α is insensitive to details of the current distribution in the wide inner region of the pipette where the series resistance is small.

These results are consistent with the transduction current being restricted to and uniformly distributed throughout the cilia. We cannot rule out intermediate current distributions, for example the possibility that the dendritic current density is non-zero but less than the ciliary current density, or that ciliary current density decreases continuously along the entire length of the cilia. However, our data show that the transduction current is not localized exclusively to the dendritic and basal ciliary membranes.

Inference from response latency

The latencies of the odorant responses in Fig. 4 provide information about the location of the transduction current if an intracellular messenger is assumed to mediate olfactory transduction. For example, if the current were localized to the dendrite, the latency of the odorant response must increase as the stimulus is displaced distally along the cilia, due to the increase in time required for the messenger to diffuse from its site of production in the cilia to ion channels in the dendrite. For second messengers such as cyclic AMP and inositol 1,4,5-trisphosphate (IP_3), which have diffusion coefficients of *ca* 5×10^{-6} cm^2 s^{-1} (estimated from their molecular weights), the latency of the odorant response would have increased by about 400 ms as the stimulus was moved 20 μm distally along the cilia. For Ca^{2+} ions, the expected delay would be about 250 ms, ignoring intracellular buffering which would increase the delay. In contrast, if the odorant-regulated channels were localized in the cilia along with the odorant binding sites, then the latency should be independent of the location of the stimulus within the cilia. The latencies of the responses of the cell of Fig. 4*B* are plotted as a function of stimulus location in Fig. 7*B*, and show that the latency does not increase significantly over a 20 μm displacement of the stimulus (similar results were obtained for the other cells in Fig. 4). This rules out localization of the odorant-induced current to the dendrite, if an intracellular messenger is a necessary step in the transduction process. It also rules out diffusion of an activated odorant receptor from the cilia to the dendrite, since this complex would diffuse even more slowly.

DISCUSSION

Cilia are the site of olfactory transduction

Our results show that both the receptor sites which confer odorant sensitivity and the channels which carry the transduction current are concentrated in the ciliary region of tiger salamander olfactory receptor cells. The cilia must therefore contain all intervening components of the transduction mechanism, because the data in Fig. 7

rule out diffusion of intracellular messengers or other molecules between the cilia and dendrite. This conclusion is consistent with a role for the second messengers cyclic AMP and IP_3 in olfactory transduction, since all of the components necessary for these second messenger pathways are present or concentrated in the cilia, i.e. the enzymes adenylyl cyclase (Pace, Hanski, Salomon & Lancet, 1985; Shirley, Robinson, Dickinson, Aujla & Dodd, 1986; Sklar, Anholt & Snyder, 1986; Boekhoff, Tareilus, Strotmann & Breer, 1990) and phospholipase C (Boyle, Park, Huque & Bruch, 1987; Boekhoff *et al.* 1990), G_{olf}, a G-protein which may link the adenylyl cyclase to odorant receptor proteins (Jones & Reed, 1989; Menco, 1991), and ion channels gated by cyclic AMP (Nakamura & Gold, 1987) and IP_3 (Restrepo, Miyamoto, Bryant & Teeter, 1990).

The close alignment between the odorant-sensitive region and the ciliary region (Fig. 4), as well as the close agreement between the ciliary and whole-cell current (Fig. 6), are consistent with transduction occurring exclusively in the cilia, although we cannot rule out a small contribution from the dendrite to the total odorant sensitivity of a cell (less than about 20%, based on the observed sensitivity profiles in Fig. 4 and less than 10% based on the equality of the suction electrode and whole-cell currents in Fig. 6*A*). This conclusion may appear to contradict the findings of Getchell *et al.* (1980) who concluded from the latency of the EOG that odorant sensitivity is restricted to the dendrite or only the basal portions of the cilia. However, their approach was based on the assumption that the latency of the EOG primarily reflected the time required for odorants to diffuse through the olfactory mucus to the receptive sites. In view of more recent observations that the intrinsic latency of olfactory transduction in amphibians is several hundred milliseconds (Firestein & Werblin, 1989), and is therefore similar to the EOG latency, diffusion of odorants through the olfactory mucus can account for only a small fraction of the EOG latency. Therefore, the data of Getchell *et al.* (1980) are consistent with the conclusions of this paper.

The linear increase in response amplitude as a function of the length of the cilia exposed to an odorant stimulus is most parsimoniously explained by assuming that the local odorant sensitivity is constant throughout the cilia and also that the cilia are electrotonically compact, even during a suprathreshold stimulus. Uniform odorant sensitivity suggests that all components of the transduction mechanism are uniformly distributed throughout the cilia. This conclusion differs from that of Adamek *et al.* (1984) who concluded that odorant sensitivity in the distal parts of frog cilia is lower than in the basal parts, based on the observation that, after deciliation, odorant sensitivity recovered to control levels before the cilia had regrown to control lengths. This discrepancy could reflect either a species difference or the failure of our technique to detect a continuous gradient in local sensitivity along the cilia. However, it is also possible that the spatial distribution of odorant sensitivity during recovery from deciliation may not reflect that which exists in mature cilia. Thus, our data may provide more direct information regarding the distribution of odorant sensitivity which normally exists *in vivo*.

Our data do not provide an explanation for the variable effects of deciliation cited in the introduction. This variability could reflect a species difference since the two studies in which deciliation was ineffective were carried out on fish (Concalon, 1980;

Kashiwayanagi *et al.* 1988), whereas the two studies in which it was effective were carried out on frogs (Bronshtein & Minor, 1977; Adamek *et al.* 1984). However, this explanation seems unlikely since several putative components of the transduction mechanism have been localized to catfish olfactory cilia (Boyle *et al.* 1987; Restrepo *et al.* 1990). In view of the complications inherent with the deciliation approach, this issue might best be resolved by using the methods described here to investigate the spatial distribution of odorant sensitivity in fish olfactory receptor cells.

Relationship between the receptor cell current and the EOG

The spatial distribution and magnitude of the currents observed in olfactory receptor cells provide direct evidence supporting the hypothesis that these currents underlie the EOG (Ottoson, 1956). That is, we have shown that odorant stimulation causes an inward ciliary current which depolarizes the cell membrane, causing an outward current through voltage-dependent conductances in the soma. This distribution is consistent with the EOG, both in sign (negative on the apical side of the epithelium) and in magnitude. The latter can be shown by using Ohm's law to calculate the transepithelial potential from the somatic current and the resistivity of the epithelium. Data are available to complete this calculation for the bull-frog, in which we have observed somatic currents as large as 22 pA (G. Lowe and G. H. Gold, unpublished observations) and in which the epithelial resistivity is 67 Ω cm^2 (Persaud, DeSimone, Getchell, Heck & Getchell, 1987). We estimate a cell density of 7×10^6 cm^{-2}, based on a count of 2×10^6 receptor neurones per olfactory nerve (Burton, 1985), and an area of 0·3 cm^2 for the sensory epithelium in one nasal cavity. Consequently, the magnitude of the somatic current predicts a maximal EOG amplitude of about 10 mV. This is greater than the maximal EOG amplitude (6 mV) observed in bull-frog in response to single odorants (Lowe, Nakamura & Gold, 1989), probably because a single odorant cannot maximally stimulate all receptor cells.

Intra-epithelial voltage measurements indicate that the current sinks of the EOG are concentrated at or above the apical surface of the epithelium, where the cilia are located, and that the current sources are concentrated in the basal part of the epithelium, where the somata are located (Ottoson, 1956; Getchell, 1977). The lower density of current sources in the dendritic layer could be due, in part, to the small diameter of the dendrite, if ion channel density is uniform throughout the dendrite and soma. However, it is also possible that the channel density is lower in the dendrite than the soma, as suggested by Fig. 4*A* and *C* where the detectable resting K^+ conductance did not extend along the entire length of the dendrite. The fact that the resting K^+ conductance extends to the tip of the dendrite in some cells but not others may reflect variations in the spatial equilibration of the resting K^+ channels following dissociation. Structures at the bases of the cilia appear to provide a more robust barrier to the movement of ion channels, since K^+-induced currents were not observed in the cilia.

Effect of membrane potential on the odorant-induced inward current

The amplitude of the transduction current was considerably smaller when the membrane potential was unclamped, than it was under voltage clamp near the resting potential (*ca* 6-fold smaller in Fig. 1, and a range of 5- to 10-fold smaller in

other experiments). This effect of membrane potential may be due to both the voltage dependence of the transduction current (Trotier, 1986; Firestein & Werblin, 1989; Kurahashi, 1989), and the much lower resistance which is in series with the ciliary conductance during voltage clamp. Another effect of membrane potential was that the time course of the response was shorter under voltage clamp at -70 mV than under current clamp (compare the whole-cell current with the suction electrode currents in Fig. 1). Assuming that the transduction mechanism involves an intracellular messenger, this suggests that membrane potential influences the metabolism of the messenger. Membrane depolarization could prolong the duration of the response by decreasing the driving force for calcium influx across the plasma membrane. This hypothesis is consistent with the observation that removing extracellular calcium abolishes adaptation to prolonged odorant stimulation (Kurahashi & Shibuya, 1990). An analogous phenomenon has been observed in vertebrate photoreceptors (Matthews, Murphy, Fain & Lamb, 1988; Nakatani and Yau, 1988).

Specializations of sensory cilia

The lower density of the resting K^+ conductance in the cilia compared with the dendrite and soma is a potentially important specialization of the cilia, because this would maximize the ciliary electrotonic length, and therefore the fraction of the transduction current which could depolarize the cell body. Due to the limited resolution of the suction electrode measurements, we can only conclude that the resting K^+ conductance per unit membrane area in the cilia is at least 5 times smaller than in the dendrite. However, in view of the very small magnitude of the rod outer segment conductance, excluding the cyclic GMP-gated conductance (Baylor & Lamb, 1982; Baylor, Matthews & Nunn, 1984), it is likely that the resting ciliary conductance may also be quite small. This observation adds to the known similarities between vertebrate photoreceptor outer segments and olfactory cilia: (1) both are based on an axonemal structure, (2) both contain cyclic nucleotide-gated conductances, and (3) both exclude ion channels which are present in the remainder of the cell. These similarities support the hypothesis of an evolutionary relationship between visual and olfactory receptor cells (Vinnikov, 1965). Molecular biological evidence for such a relationship is provided by the recent cloning of the olfactory cyclic nucleotide-gated channel, based on its sequence similarity with the rod cyclic GMP-gated channel (Dhallan, Yau, Schrader & Reed, 1990).

Evidence that odorants diffuse rapidly through the olfactory epithelium

It is well known that most volatile odorants are hydrophobic, and may therefore diffuse across cell membranes into the olfactory epithelium. The hydrophobicity of odorants reflects the fact that, in order to be volatile, odorants cannot be strongly polar or ionic molecules. Diffusion of odorants into the olfactory epithelium has been invoked to provide a function for oxidizing enzymes in the supporting cells, i.e. these enzymes could assist in the clearance of odorants from the olfactory epithelium (Lazard, Tal, Rubinstein, Khen, Lancet & Zupko, 1990). Our finding that odorants can rapidly diffuse across the receptor cell membranes supports this hypothesis and

demonstrates that movement of odorants through the olfactory epithelium may be fast enough to influence the dynamics of odorous stimuli.

We thank L. M. Masukawa, R. A. Maue and E. N. Pugh Jr for valuable comments on the manuscript, and T. Getchell for providing a translation of Bronshtein & Minor (1977). This work was supported by U.S. N.I.H. grant DC00505.

REFERENCES

ADAMEK, G. D., GESTELAND, R. C., MAIR, R. G. & OAKLEY, B. (1984). Transduction physiology of olfactory receptor cilia. *Brain Research* **310**, 87–97.

BADER, C. R., MACLEISH, P. R. & SCHWARTZ, E. A. (1979). A voltage-clamp study of the light response in solitary rods of the tiger salamander. *Journal of Physiology* **296**, 1–26.

BAYLOR, D. A. & LAMB, T. D. (1982). Local effects of bleaching in retinal rods of the toad. *Journal of Physiology* **328**, 49–71.

BAYLOR, D. A., LAMB, T. D. & YAU, K.-W. (1979). The membrane current of single rod outer segments. *Journal of Physiology* **288**, 589–611.

BAYLOR, D. A., MATTHEWS, G. & NUNN, B. J. (1984). Location and function of voltage-sensitive conductances in retinal rods of the salamander, *Ambystoma tigrinum*. *Journal of Physiology* **354**, 203–223.

BOEKHOFF, I., TAREILUS, E., STROTMANN, J. & BREER, H. (1990). Rapid activation of alternative second messenger pathways in olfactory cilia from rats by different odorants. *EMBO Journal* **9**, 2453–2458.

BOYLE, A. G., PARK, Y. S., HUQUE, T. & BRUCH, R. C. (1987). Properties of phospholipase C in isolated olfactory cilia from the channel catfish (*Ictalurus punctatus*). *Comparative Biochemistry and Physiology* B **88**, 767–775.

BRONSHTEIN, A. A. & MINOR, A. V. (1977). The regeneration of olfactory flagella and restoration of electroolfactogram after the treatment of the olfactory mucosa with Triton X-100. *Tsitologiya* **19**, 33–39.

BURTON, P. R. (1985). Ultrastructure of the olfactory neuron of the bullfrog: the dendrite and microtubules. *Journal of Comparative Neurology* **242**, 147–160.

CONCALON, P. (1980). Effect of salts, pH and detergents on the catfish olfactory mucosa. In *Proceedings of the Seventh International Symposium on Olfaction and Taste*, ed. VAN DER STARRE, H., pp. 73–76. Information Retrieval Inc., New York.

DHALLAN, R. S, YAU, K.-W., SCHRADER, K. A. & REED, R. R. (1990). Primary structure and functional expression of a cyclic nucleotide-activated channel from olfactory neurons. *Nature* **347**, 184–187.

FIRESTEIN, S., SHEPHERD, G. M. & WERBLIN, F. S. (1990). Time course of the membrane current underlying sensory transduction in salamander olfactory receptor neurons. *Journal of Physiology* **430**, 135–158.

FIRESTEIN, S. & WERBLIN, F. (1989). Odor-induced membrane currents in vertebrate-olfactory receptor neurons. *Science* **244**, 79–82.

GETCHELL, T. V. (1977). Analysis of intracellular recordings from salamander olfactory epithelium. *Brain Research* **123**, 275–286.

GETCHELL, T. V., HECK, G. L., DESIMONE, J. A. & PRICE, S. (1980). The location of olfactory receptor sites. Inferences from latency measurements. *Biophysical Journal* **29**, 397–472.

HAMILL, O. P., MARTY, E., NEHER, B., SAKMANN, B. & SIGWORTH, F. J. (1981). Improved patch-clamp techniques for high resolution current recording from cells and cell-free membrane patches. *Pflügers Archiv* **391**, 85–100.

JONES, D. T. & REED, R. R. (1989). G_{olf}: an olfactory neuron specific-G protein involved in odorant signal transduction. *Science* **244**, 790–795.

KASHIWAYANAGI, M., SHOJI, T. & KURIHARA, K. (1988). Large olfactory responses of the carp after complete removal of olfactory cilia. *Biochemical and Biophysical Research Communications* **154**, 437–442.

KLEENE, S. J. & GESTELAND, R. C. (1983). Dissociation of frog olfactory epithelium. *Journal of Neuroscience Methods* **9**, 173–183.

KURAHASHI, T. (1989). Activation by odorants of cation-selective conductance in the olfactory receptor cell isolated from newt. *Journal of Physiology* **419**, 177–192.

KURAHASHI, T. & SHIBUYA, T. (1990). Ca^{2+}-dependent adaptive properties in the solitary olfactory receptor cell of the newt. *Brain Research* **515**, 261–268.

LAZARD, D., TAL, N., RUBINSTEIN, M., KHEN, M., LANCET, D. & ZUPKO, K. (1990). Identification and biochemical analysis of novel olfactory-specific cytochrome P-450IIA and UDP-glucuronyl transferase. *Biochemistry* **29**, 7433–7440.

LOWE, G., NAKAMURA, T. & GOLD, G. H. (1989). Adenylate cyclase mediates transduction for a wide variety of odorants. *Proceedings of the National Academy of Sciences of the USA* **86**, 5641–5645.

MATTHEWS, H. R., MURPHY, R. L. W., FAIN, G. L. & LAMB, T. D. (1988). Photoreceptor light adaptation is mediated by cytoplasmic calcium concentration. *Nature* **334**, 67–69.

MENCO, B. PH. M. (1991). Ultrastructural localization of the transduction apparatus in the rat's olfactory epithelium. In *Abstract book of Association for Chemoreception Sciences*, No. 171.

NAKAMURA, T. & GOLD, G. H. (1987). A cyclic nucleotide-gated conductance in olfactory receptor cilia. *Nature* **325**, 442–444.

NAKATANI, K. & YAU, K.-W. (1988). Calcium and light adaptation in retinal rods and cones. *Nature* **334**, 69–71.

OTTOSON, D. (1956). Analysis of the electrical activity of the olfactory epithelium. *Acta Physiologica Scandinavica* **35**, suppl. 122, 1–83.

PACE, U., HANSKI, E., SALOMON, Y. & LANCET, D. (1985). Odorant-sensitive adenylate cyclase may mediate olfactory reception. *Nature* **316**, 255–258.

PERSAUD, K. C., DESIMONE, J. A., GETCHELL, M. L., HECK, G. L. & GETCHELL, T. V. (1987). Ion transport across the frog olfactory mucosa: the basal and odorant-stimulated states. *Biochimica et Biophysica Acta* **902**, 65–79.

REESE, T. S. (1965). Olfactory cilia in the frog. *Journal of Cell Biology* **25**, 209–230.

RESTREPO, D., MIYAMOTO, T., BRYANT, B. & TEETER, J. H. (1990). Odor stimuli trigger influx of calcium into olfactory receptor neurons. *Science* **249**, 1166–1168.

SHIRLEY, S. G., ROBINSON, C. J., DICKINSON, K., AUJLA, R. & DODD, G. H. (1986). Olfactory adenylate cyclase of the rat. Stimulation by odorants and inhibition by Ca^{2+}. *Biochemical Journal* **240**, 605–607.

SKLAR, P. B., ANHOLT, R. R. H. & SNYDER, S. H. (1986). The odorant-sensitive adenylate cyclase of olfactory receptor cells. Differential stimulation by distinct classes of odorants. *Journal of Biological Chemistry* **261**, 15538–15543.

STUHMER, W., ROBERTS, W. M. & ALMERS, W. (1983). The loose patch clamp. In *Single Channel Recording*, ed. SAKMANN, B. & NEHER, E. Plenum Press, New York.

TROTIER, D. (1986). A patch-clamp analysis of membrane currents in salamander olfactory receptor cells. *Pflügers Archiv* **407**, 589–595.

VINNIKOV, J. A. (1965). Principles of structural, chemical, and functional organization of sensory receptors. *Cold Spring Harbor Symposia on Quantitative Biology* **30**, 293–300.